Available online at www.sciencedirect.com
SCIENCE DIRECT®
International Journal of Heat and Fluid Flow 26 (2005) 709–721
International Journal of HEAT AND FLUID FLOW
www.elsevier.com/locate/ijhff

An experimental investigation of fluid flow and wall temperature distributions in an automotive headlight

J.M.M. Sousa [a,*], J. Vogado [a], M. Costa [a], H. Bensler [b], C. Freek [b], D. Heath [c]

[a] *Instituto Superior Técnico, Department of Mechanical Engineering, Av. Rovisco Pais, 1049-001 Lisboa, Portugal*
[b] *Volkswagen AG, D-38436 Wolfsburg, Germany*
[c] *Ricardo GmbH, D-38444 Wolfsburg-Hattorf, Germany*

Received 11 October 2004; received in revised form 12 February 2005; accepted 15 May 2005
Available online 11 July 2005

Abstract

Detailed measurements of wall temperatures and fluid flow velocities inside an automotive headlight with venting apertures are presented. Thermocouples have been used to characterize the temperature distributions in the walls of the reflectors under transient and steady operating conditions. Quantification of the markedly three-dimensional flow field inside the headlight cavities was achieved through the use of laser-Doppler velocimetry for the latter condition only. Significant thermal stratification occurs in the headlight cavities. The regime corresponding to steady operating conditions is characterized by the development of a vortex-dominated flow. The interaction of the main vortex flow with the stream of colder fluid entering the enclosed volume through the venting aperture contributes significantly to increase the complexity of the basic flow pattern. Globally, the results have improved the understanding of the temperature loads and fluid flow phenomena inside a modern automotive headlight.

Keywords: Automotive headlight; Headlamp cavity; Natural convection; Internal heat source; Wall temperature; Laser-Doppler velocimetry

1. Introduction

In recent years, extensive changes have been introduced in the design of automotive front lighting systems. Some of these changes are clearly visible, but there have also been more subtle transformations conferring additional functions to modern automotive headlights such as adaptive lighting capabilities. On the other hand, lighting systems have evolved from a nearly exclusive technical purpose to become an integral component of vehicle styling. This has brought into play various conflicts, namely technical requirements versus styling aspects and innovation versus regulations (Huhn, 2002). In particular, the demand for more compact designs, employing lightweight and recycling materials, has made the task of achieving thermal performance in headlights more and more difficult to fulfill.

The use of lightweight materials in headlight assemblies has allowed manufacturers to compensate for the increase in weight imposed by the growing complexity in design. The replacement of glass by semi-transparent polycarbonate in the front lens of a headlight is perhaps the most conspicuous example of this practice. Moreover, the use of molded plastic compounds in headlight assemblies is the rule nowadays. As the application of these materials is constrained by limited ranges of temperature, temperature loads in the headlight must be carefully taken into account in the design process. The consequences of unsuitable choices made at this stage include long-term damage to various plastic parts due to high-temperature stresses and a reduction of the light

* Corresponding author. Tel.: +351 21 841 7320; fax: +351 21 849 5241.
E-mail address: msousa@alfa.ist.utl.pt (J.M.M. Sousa).

0142-727X/$ - see front matter © 2005 Elsevier Inc. All rights reserved.
doi:10.1016/j.ijheatfluidflow.2005.05.003

Nomenclature

g	gravitational acceleration
k	thermal conductivity
L	length scale of the cavity
Q	volumetric heat source
Ra	Rayleigh number, $g\beta\Delta TL^3/(\alpha\nu)$
Ra'	modified Rayleigh number, $g\beta QL^5/(\alpha\nu k)$
T	time-averaged temperature
U, V, W	time-averaged velocity components of the fluid
X, Y, Z	space coordinates

Greeks

α	thermal diffusivity
β	thermal expansion coefficient
ν	kinematic viscosity

Subscripts

amb	ambient
max	maximum

bulbs lifespan. This potentially results in poor lighting performance and, eventually, premature failure of the headlight.

Another important aspect to take into consideration is the fact that, contrary to older-style headlights, modern plastic-made headlight assemblies are not hermetically manufactured. Venting apertures are usually installed in order to allow for expansion and contraction as the air within the light chamber heats and cools. However, this also means that air is permitted to be exchanged with the atmosphere. As a result, moisture may enter and, given the appropriate conditions, condense on internal surfaces. This is undesirable as it may have an impact on both the normal operation of the headlight (e.g., compromising the beam pattern, oxidizing electrical connections) and on its aesthetic appearance (Bielecki et al., 2003). On the other hand, sensible placement of the venting apertures may generate an airflow pattern that sweeps away the condensation in a very efficient manner as the headlight warms up. Additionally, stagnant internal fluid areas can be minimized and a clever design will also take advantage of this airflow to cool down the hot parts.

Nevertheless, the main flow inside a headlight is not generated by the vents. The presence of thermal sources (i.e., the light bulbs) inside the headlight cavities gives rise to the establishment of internal buoyancy-driven circulations. Similarly, and on the topic of electronic components packaged within an enclosure (see a review by Incropera, 1988), buoyancy forces induce a recirculating flow within the enclosed space and heat transfer occurs by natural convection. However, the role of conduction and, especially, radiative heat transfer cannot be disregarded in the analysis of the present case. The interaction of the aforementioned recirculating flow pattern with the stream of external air entering the vents, and the geometric intricacy of modern headlight casings, further contribute to the increased complexity of this subject.

The investigation of natural convection in porous cavities with internal heat generation has received particular attention in the last few years as a consequence of its wide range of applications (many references; see e.g. Jue, 2003). However, the fundamental physics of the foregoing subject differ significantly from that of simple air-filled (no porous material) enclosures containing internal thermal sources. For the latter class of problems, Yerkes and Faghri (1992) determined the effects of mixed convection on the flow structure of large baffled chambers. Sun and Emery (1997) studied the effects of wall conduction, internal heat sources and a baffle on natural convection heat transfer in a rectangular box. More recently, a two-dimensional enclosure containing internal heating elements (either two vertical plates or a rectangular block) was investigated numerically by Barozzi and Corticelli (2000). These three examples provide relevant information for the understanding of fluid flow and heat transfer phenomena in vented automotive headlights but still constitute crude simplifications of the actual physical scenario.

Successful attempts to numerically simulate automotive headlights have been made by Moore and Powers (1999) and Moore et al. (1999), using finite element analysis methods for solving coupled specular radiation and natural convection with an unstructured computational mesh. Recent simulations, also employing sophisticated computational fluid dynamics (CFD) tools, have been carried out by Chenevier (2001), Wulf and Reich (2002) and Halgren and Hilburger (2003). In addition, Shiozawa et al. (2001) and Okada et al. (2002) have presented CFD predictions together with very limited measurements of fluid flow inside the headlight (in a plane adjacent to the surface of the lens only) using particle image velocimetry (PIV). Overall, these studies have shown that a good correlation between simulations and experiments can nowadays be obtained. However, it is evident that the success of the aforementioned numerical simulations relies heavily on the availability of detailed experiments. Hence, the scarcity of experimental data and the need for a better

understanding of the underlying mechanisms have provided the grounds for the accomplishment of the present study.

In this investigation, detailed wall temperature measurements in the reflectors of an automotive headlight have been carried out employing thermocouples. These have been performed both during warm-up and at steady operating conditions. A distinctive feature of the present work is that it also includes the measurement of fluid flow velocities inside the headlight cavities. These have been obtained using a three-component set-up of a laser-Doppler velocimeter, which provided a quantitative characterization of the buoyancy-induced circulations inside the enclosure.

2. Experimental apparatus and procedures

In this section a detailed description of the headlight characteristics and measuring techniques employed in the course of the present investigations is given. Uncertainty estimates for wall temperature and fluid flow velocity measurements are also provided.

2.1. Headlight characteristics

A driver's side headlight from a Volkswagen Polo (year 2002; continental Europe) was employed in the present investigations (Fig. 1a). This unit is part of the vehicles' quad-beam front lighting system. It is designed with single housing (Fig. 1b) for the multiple bulb assembly and a clear double lens (Fig. 1c). It includes low- and high-beam lamps, turn-signal lamp and parking lamp (inside the high-beam cavity). The main reflector (Fig. 1d) is constructed according to the Free-Form technique, which makes use of computer-aided lighting to optimize the shape of the reflector surface and bulb position. As a result, the desired beam pattern may be solely generated by the shape of the reflector, without requiring additional optical elements and leaving the crystal clear cover lens with a purely protective function. Secondary reflectors with integrated bezel are used in the high- (Fig. 1e) and low-beam (Fig. 1f) assemblies as well. A ribbed horizontal divider in the low-beam secondary reflector demarcates the cavity for the turn-signal light, which combines reflector and Fresnel optics. The high-beam part of the cluster is thus formed by the left-hand

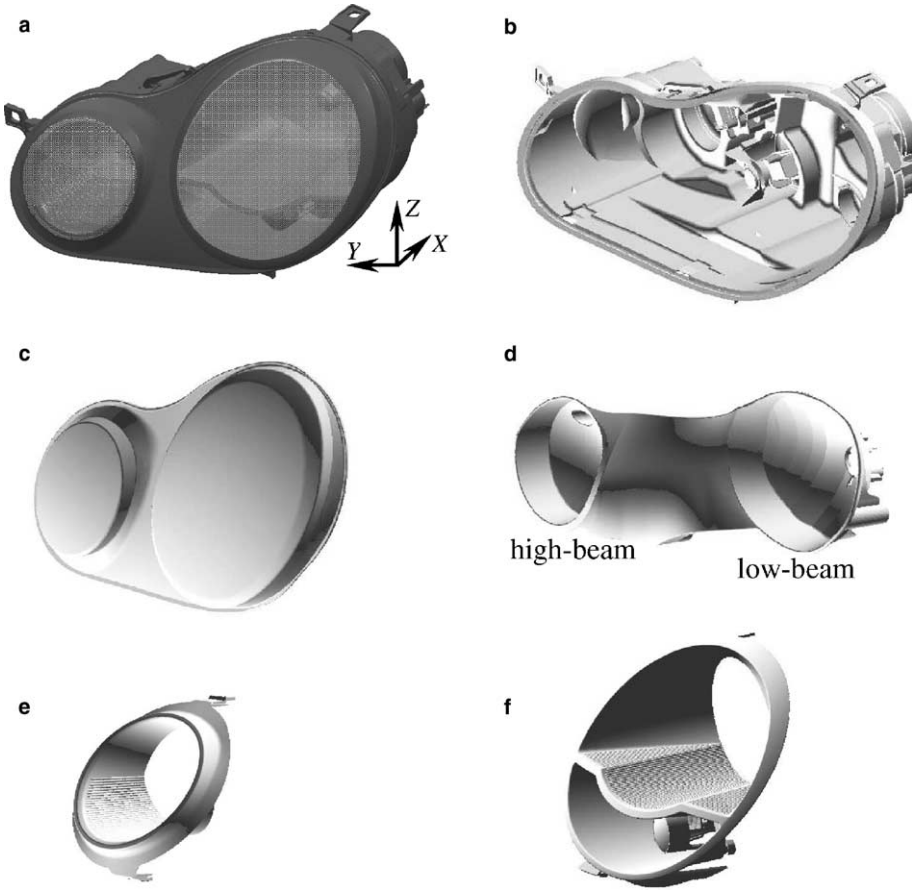

Fig. 1. Automotive headlight. (a) Complete assembly and coordinate system, (b) casing, (c) front lens, (d) main reflector, (e) secondary reflector of the high-beam, and (f) secondary reflector of the low-beam.

side concave surface of the main reflector (Fig. 1d) together with the corresponding secondary reflector (Fig. 1e), whereas the low-beam part is formed by the right-hand side concave surface of the main reflector (Fig. 1d) together with the upper part (up to the horizontal divider) of the corresponding secondary reflector (Fig. 1f).

Halogen bulbs are utilized in the principal lighting components of the headlight. Halogen lamps are brighter (about 25%) and last longer than standard incandescent lamps because the bulbs contain a small amount of bromine gas. This extends the life of the bulb and prevents the glass from darkening as the bulb ages. Conventional incandescent bulbs are used for the remaining lighting components.

A digital power supply was employed to apply a constant voltage of 13.2 V to the bulbs. Measurements of input current values indicated that this operating condition leads to an excess of about 10% over reference power ratings. All investigations have been carried out with the simultaneous operation of low- and high-beams only. For this purpose, the headlight was mounted in operating position using an appropriate structure and was held stationary in a quiescent environment. This fact should not be seen as a shortcoming of the present results because the presence of forced convection over the front lens would introduce additional uncertainties to the study.

The headlight casing has four venting apertures aiming to allow the exchange of mass between (hotter) internal air and (cooler) environmental air. Two of these vents potentially operate as inlets, whereas the other two may be considered as potential outlets. During the present study only two of these vents were kept open, as shown in Fig. 2. The larger openings seen in the back of the headlight are intended for servicing only and these remained sealed by the use of suitable plastic and rubber caps. High- and low-beam cavities communicate laterally through the existing gaps between the secondary reflectors and the main reflector. Additionally, these gaps allow the exchange of mass between the air inside the cavities and the remaining internal air contained in the housing where the vents are installed.

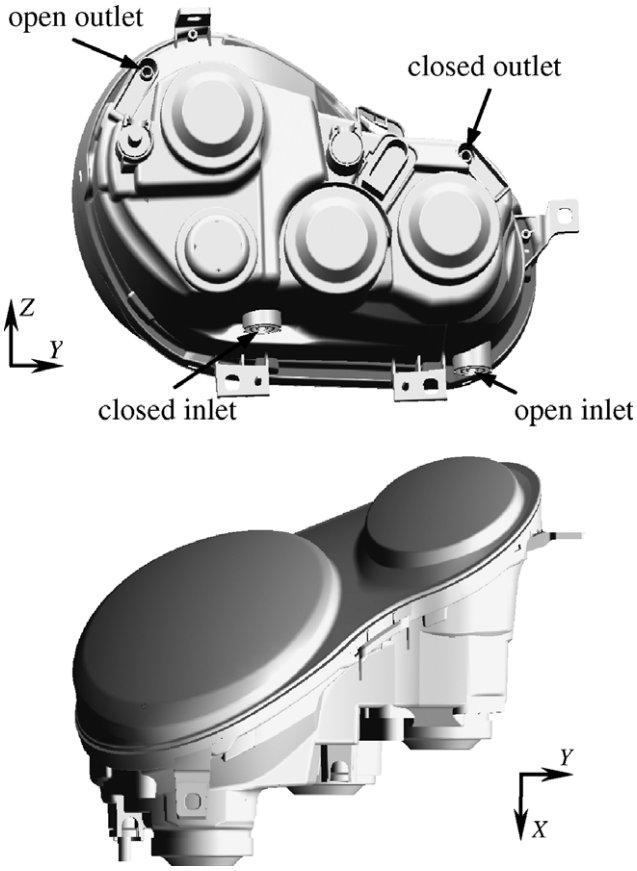

Fig. 2. Venting apertures in the headlight.

2.2. Wall temperature measurements

The tungsten filaments in halogen bulbs can reach temperatures higher than 3000 K. These heat sources emit radiation and most of it is transmitted through the bulb filling gas and glass to the inner surfaces of the headlights as visible and infrared radiation (Küpper and Schug, 2002). Heat losses to the bulb glass induce the natural convection of air inside the headlights. On the other hand, high-performance reflective surfaces provide a near-specular reflection of the incident radiation within the headlight. A significant amount of this radiation is then transmitted through the front lens to the environment. However, it must also be noted that a very significant portion of the energy released is absorbed by the headlight components, thus leading to a temperature increase of these parts. Fortunately, a fraction of this energy is transferred via conduction to the outer surfaces of the casing where it is mainly convected and radiated to the surrounding media. Despite this mechanism, high temperature may still be reached in some regions of the headlight, thus restricting the choice of materials and affecting the lifespan of the various components. It can be anticipated that, due to close proximity of the heat sources, the reflectors are thermally problematic parts.

A systematic campaign of wall temperature measurements in the reflectors was performed using thermocouples. Infrared measurements were not applied here as a consequence of limited optical access. This technique is usually employed in this context to seek for "hot spots" on external surfaces only. Further, taking into account the multitude of sources for inaccuracy intrinsic in the use of infrared sensors in this situation (e.g., uncertain emissivity values, non-planar surfaces, parasitic radiation from other components), the accuracy provided by thermocouples constitutes a better option.

Following the definition of a measurement grid over the back surface of the reflectors defining 98 measure-

ment locations, more than 100 type-T, bare-wire (beaded) thermocouples have been manufactured. Thermocouple joints were obtained by welding the two constituent wires (0.3 mm in diameter) after a very short twist. This improves the mechanical durability of the joint without significantly compromising the sensitivity and accuracy of the thermocouple. The resulting beads were approximately 0.7 mm wide.

In order to embed each of the thermocouple beads in the reflector material, it was necessary to drill appropriate cavities. This was achieved in two steps. Firstly, a pass-through hole was made using a drill 0.75 mm in diameter. Thereafter, a second hole with a diameter of 1.25 mm was drilled from the back of the reflector up to a certain depth only. The depth of the secondary hole varied according to the local thickness of the material, which in turn varied between 2 and 4 mm. This procedure allowed not only to ease the insertion (and replacement if needed) of the thermocouple beads into the walls of the reflectors but also permitted the thermocouple beads to be mounted flush with the inner reflector surface. In addition, the back of the passage was sealed and the thermocouple cables were fixed to the back surface of the reflectors using temperature-resistant silicon glue.

Following the installation of all thermocouples in the reflectors, the headlight was reassembled. Front lens gaps and slits made on the service caps, used for the passage of the thermocouple cables, were also sealed (using the same silicon glue). Thermocouple connections were accomplished using two breadboards, permitting fast scanning through all measurement points. For the measurements, a portable PC was interfaced with a T-type board model 5B47-T from DATA TRANSLATION, employing a USB board model DT9802 supplied by the same manufacturer. In turn, the T-type board was linked to the connection breadboards using compensating grade wire.

Both steady state and transient measurements of wall temperatures have been carried out. The latter were performed first in order to establish the heat-up time required for the headlight to achieve a steady operating condition. In both cases, the software HP VEE Lab was employed for data acquisition.

2.3. Fluid flow velocity measurements

As mentioned in the previous subsection, the hot surfaces inside the headlight induce natural convection. The geometrical complexity gives rise to the establishment of an intricate flow pattern, which is further complicated by the presence of the air stream through the venting apertures. The recirculating flow inside the headlight cavities demands the use of a non-intrusive accurate measurement technique. Previous attempts to visualize the flow using light-sheet illumination have shown that the application of an image-based flow measurement technique (such as PIV) without making major modifications to the headlight would face extreme difficulties. Even the use of a polarization filter to minimize the effect of parasitic reflections does not improve the image to an acceptable quality. As a consequence, laser-Doppler velocimetry (LDV) was the technique chosen to carry out the quantitative characterization of the flow behavior in the above-mentioned areas.

Three velocity components have been measured in various planes inside the headlight cavities using an LDV system from DANTEC operated in backward scattering mode. The full system consists of a coherent light source, transmission optics (including acousto-optic modulator for elimination of directional ambiguity and color splitter), receiving optics and detectors (photomultipliers), and signal conditioners/processors. The laser source was a 3-W (nominal) Ar-ion laser from COHERENT. In the present configuration, two fiberoptic probes equipped with biconvex lenses (focal distance of 400 mm) were utilized as receptors of the scattered light. A so-called 2D probe was employed to measure two velocity components using the green and blue laser pairs of beams. A second probe, denominated 1D, allowed the measurement of the third velocity component using the violet pair.

Ideally, all three planes containing the pairs of laser beams should have normals which are mutually perpendicular. This has been possible using the 2D probe only. Due to geometrical restrictions, the 1D probe cannot generally be placed at an angle of 90° with the other probe. Typical angles are 30–45°. The coordinate transformation methodology (Albrecht et al., 2003) allowed determination of the third velocity component (in a direction perpendicular to the remaining components) and was subsequently carried out by software. Unfortunately, this procedure introduces errors in the quantification of this velocity component: the smaller the angle, the larger the associated error. In the present study, two different geometrical arrangements were used for the fiberoptic probes, as illustrated in Fig. 3. By changing the position of the probes from one side to the other, instead of using the (traditional) symmetrical configuration, it was possible to maximize the angle between them. Hence, even measuring locations placed far back in the vicinity of the bulbs could be accessed without incurring a too greater reduction of the angle. A value of 20° chosen for the angle between the probes is the result of the compromise between these two objectives.

Both fiberoptic probes were mounted on a rigid, computer-controlled traversing system from ISEL Automation, allowing movements in the three coordinate directions. The electronic mechanism assures a spatial accuracy of ± 100 μm. One should also note that, in order to obtain accurate measurements, the laser beams cannot suffer significant deviations when crossing the

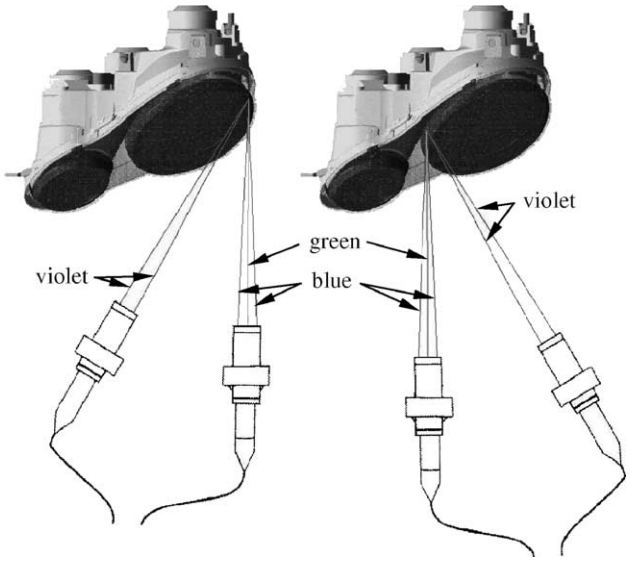

Fig. 3. Geometrical arrangements of the LDV fiberoptic probes.

media. In the case of the headlight, the beams must pass through the front lens. As mentioned previously, the lens is made of a semi-transparent plastic molded compound, presenting good homogeneity and a small thickness. Moreover, excluding the perimeter locations, there is only a mild surface curvature in the lens. A comparison between real traversing distances of the measuring volume inside the headlight cavities and design dimensions was conducted to assess the magnitude of optical deviations. It was concluded that these were acceptable throughout the entire set of measurements (see also Section 2.4).

The backward scattered light captured by the receptors located in the fiberoptic probes was separated into the three original colors using interference filters. Subsequently, the light received was converted into electric signals by the photomultipliers. The entire signal processing, which included pedestal removal and filtering, was performed by three ''Burst Spectrum Analysers'', models 57N20/57N35 from DANTEC. The final processing of the data was carried out by the BURSTware software version 3.11, also from DANTEC. Data management was attained by the use of this software as well, which further allowed the control and automation of the measurements. The quality of the analog signal was monitored employing a four-channel oscilloscope.

LDV measurements require seeding with adequate characteristics, namely good scattering properties and the ability to follow the flow. The use of a backward scattering configuration is particularly demanding in terms of seeding, as the intensity of the light scattered by the particles in this direction is usually much smaller. On the other hand, the concentration of seeding particles must be controlled with respect to density and homogeneity. Based on previous experience, it was decided to use the smoke produced by the combustion of small bars made of incense, resin and wood waste as seeding. However, in order to generate smoke at a controllable constant rate, maintain a steady combustion process and minimize fouling, a tailored seeding generator/feeder had to be designed.

Fig. 4 shows a schematic of this device. Although the device includes a pump and hot parts, its operation must not alter the pressure or the temperature at the venting aperture. The pump was employed to promote the flow through the piping circuit rather than to increase the pressure inside the inlet chamber. It was concluded that the use of this chamber facilitated the control of air conditions before entering the headlight. The chamber was constructed in transparent polymethyl methacrylate and the incense smoke was fed in through a flexible pipe. The resulting weak pressure increase inside the inlet chamber was further reduced by the installation of an equalizer pipe connecting it to atmospheric conditions.

Several tests were made to assess the consequences of using this feeding procedure. Velocity measurements were carried out at various key locations inside the headlight, while alternating between pump-on and -off status. This was found to have a negligible effect on the results. Moreover, the initially hot smoke was effectively cooled down before release. It was verified that the temperature of the smoke fed into the inlet chamber differed no more than 1 °C from the room temperature. As a conclusion, the device met all the above-mentioned needs in addition to the requirement of removing most of the liquid condensates. However, despite these measures, the lengthy time-span demanded to accomplish the measurement campaign called for headlight reflectors and lens to be periodically cleaned. As a consequence, a removable front lens with appropriate sealing had to be installed. Interior surfaces could thus be cleaned directly by the application of a mild solvent. However, as a result of the continued action of some agents present in the smoke, the surface of the reflectors and the lens eventually suffered chemical deterioration by their deposit. Whenever this occurred, the reflectors were replaced and the lens polished or replaced as well.

2.4. Uncertainty estimates

The number of individual velocity values utilized to evaluate time-averages, calculated by ensemble averaging, varied between 3000 (generally) and 500 in areas with lower signal-to-noise ratio (mainly located in the vicinity of the light bulb). This led to statistical (random) errors below 4% for mean quantities, according to the analysis given by Albrecht et al. (2003) for a 95% confidence level. The use of high data rates with respect to the (low) fundamental velocity fluctuation rates allowed the minimization of systematic errors, as suggested by Erdmann and Tropea (1981). Sampling bias was expected to be negligi-

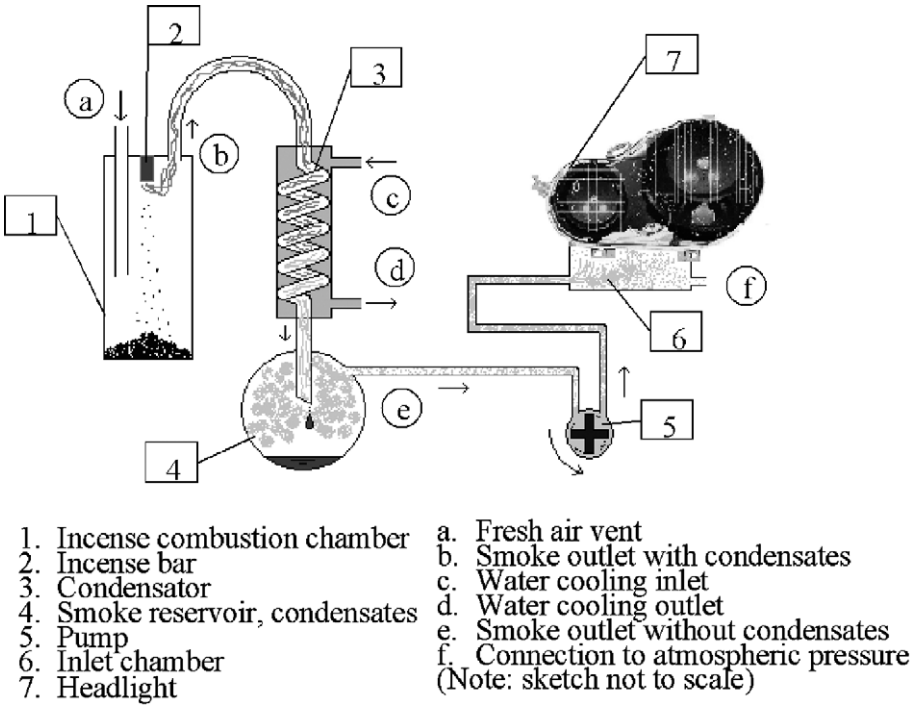

Fig. 4. Schematic of the seeding generator/feeder.

ble as a consequence of the use of particle residence time weighting on the estimation of the velocities (Buchhave et al., 1979). In addition, non-turbulent Doppler broadening errors due to gradients of mean velocity across the measuring volume mainly affect the variance of velocity fluctuations (Albrecht et al., 2003). The sizes of the principal axes describing the LDV probe volume were approximately 0.2, 0.2 and 4 mm.

Fluctuations of the fluid refractive index due to large temperature fluctuations may cause the laser beams to wander and defocus in the fluid. This corruption of laser beam properties reduces the signal-to-noise ratio levels dramatically. These effects were observed only in a few measuring locations directly above the light bulbs, where the temperature fluctuations were large enough. Whenever this occurred the data were discarded. This precluded the accomplishment of velocity measurements at the mentioned locations, which can be observed in the velocity maps corresponding to the planes crossing the light bulbs (missing vectors in the grid).

The procedure followed for the determination of the off-plane velocity component (resulting from the conjunction of in-plane and 20° off-axis measurements), led to errors approximately five times larger than those obtained for the in-plane velocity components. As a result, the various sources of errors and biases suggested an uncertainty of less than 4% for in-plane mean velocities (V, W) and 20% for the off-plane mean velocity (U). Concerning spatial accuracy, the various sources of uncertainty (systematic errors such as referencing the system with respect to the headlight and small optical deviations) indicate that the maximum spatial error in the measurement process was approximately 1 mm.

Temperature values were computed from 6000 samples, thus leading to statistical errors below 1%, according to the above-mentioned analysis (Albrecht et al., 2003). Apart from an instrumental error of less than 0.5% in measuring the electromotive force, errors can mainly arise from conduction along the thermocouple wire, radiation losses and positioning of the thermocouple bead in the reflector surface. Given the range of measured temperatures, the conduction and radiation losses for thermocouples of the present configuration are negligible. As for the positioning of the thermocouple bead for locations normal to the reflector surface, the arrangement described in Section 2.2 ensured that the thermocouple beads were mounted flush with the inner reflector surface so that the resulting uncertainties were unimportant. Data reproducibility, which is a good indicator of the accuracy of the measurements, was, on average, within 2%.

3. Results and discussion

3.1. Flow regime

Natural convection in enclosures is the result of thermal and momentum interactions between a finite-size fluid system and the confining walls. These flows may

be loosely organized (Bejan, 1984) into two large classes: Bénard-type and side-heated enclosures. The study of both cases requires the definition of a Rayleigh number based on a wall temperature difference, as follows:

$$Ra = \frac{g\beta \Delta T L^3}{\alpha v}. \quad (1)$$

In the present problem, the measured temperature difference between the walls ($\Delta T_{max} \approx 110$ K) is in fact a consequence of the presence of a heat source inside the headlight cavities. Such volumetric heat sources induce heat transfer and flow characteristics which differ from those of an externally heated enclosure. Thus, an additional parameter, namely a modified Rayleigh number that takes into account the strength of internal heating, must also be defined as follows:

$$Ra' = \frac{g\beta Q L^5}{\alpha v k}. \quad (2)$$

The strength of the internal heat source Q is known and the characteristic length scale L can be chosen as any of the principal dimensions of the headlight cavities as all of these are of the same magnitude. Hence, the approximate evaluation of the parameters expressed by Eqs. (1) and (2) for the headlight problem yields the following values: $Ra \approx 10^7$ and $Ra' \approx 10^9$. Based on the given parameters, the flow regime inside the headlight cavities is expected to be laminar, although the thermal plumes above the light bulbs may show transitional characteristics. This was confirmed during the LDV investigations by the measurement of much higher values of the velocity variances (not shown here) in these areas. Flow visualization using the seeding smoke as tracer particles has further substantiated the above view. However, the issue of the stability of the thermal plumes was not addressed in the present work.

3.2. Wall temperature distributions

Measurements of the transient temperature evolution during a long period (longer than 150 min) have been conducted in order to determine the time required for the headlight to attain steady operating conditions. Fig. 5 depicts the time traces of temperature recorded from two of the thermocouples installed in the main reflector. These are representative of the highest temperatures measured in the walls of the low- and high-beam cavities. It can be concluded that, under the investigated conditions, the headlight has a heat-up time of nearly 120 min. This is roughly the time it takes for the temperature at the examined locations (see also Fig. 6) to reach levels differing less than 0.5 °C from the stabilized values. It must be mentioned that, during these and the steady measurements, the ambient temperature T_{amb} was approximately 19.5 °C and varied less than 0.5 °C across the whole duration of the experiments.

Steady measurements have been performed allowing the headlight to warm up for a period of at least 120 min. With the aim of assessing data reproducibility, three independent sets of measurements were gathered for the same operating conditions. Time-averaged temperatures obtained from a total of 98 thermocouples installed in the main reflector, secondary reflector of the high-beam and secondary reflector of the low-beam are shown in Fig. 6a–c, respectively. In these figures the measured temperatures have been color-coded in steps of 10 °C from dark blue (lowest range) to dark red (highest range). The time-averaged air temperatures at the inlet and outlet venting apertures were also monitored during the experiments. These values were, respectively, 21.5 °C and 77.5 °C, with a range of variation similar to that of T_{amb}.

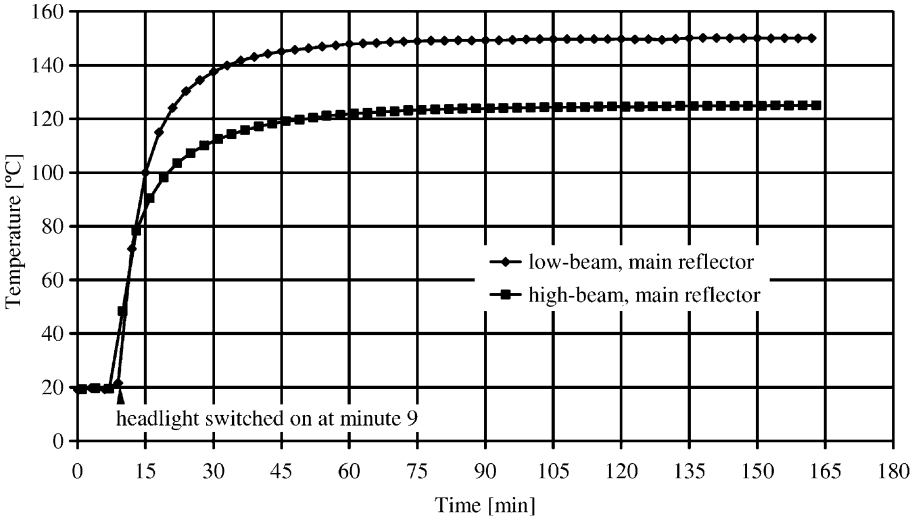

Fig. 5. Time traces of maximum wall temperatures during warm-up.

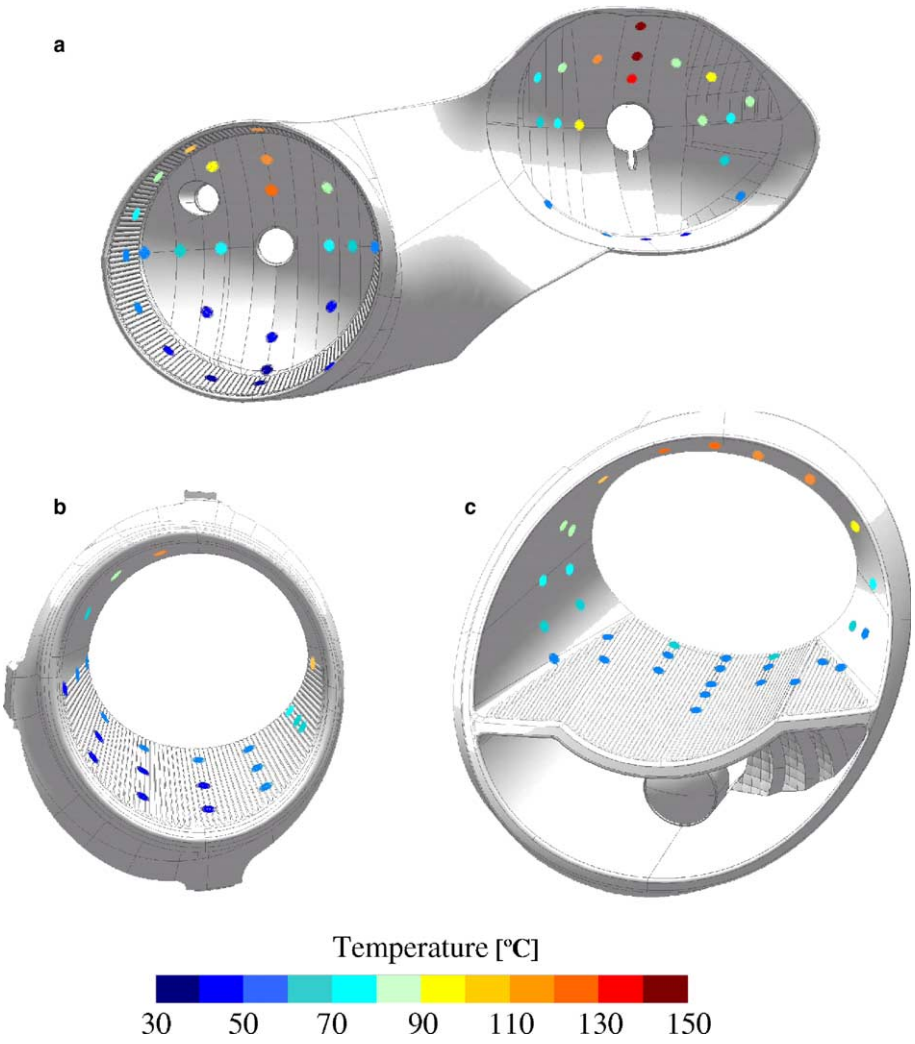

Fig. 6. Temperatures in the walls of the reflectors for steady operating conditions. (a) Main reflector, (b) secondary reflector of the high-beam, and (c) secondary reflector of the low-beam.

Fig. 6a clearly illustrates the drastic effect of the thermal plume rising from the heat sources (light bulbs) on wall temperature distributions. The highest temperatures are achieved in the regions directly above the plume, both for low- and high-beams. Moreover, the resulting stratification of the fluid is much more pronounced in the upper halves of the cavities than on the remaining space. Somewhat surprisingly, the temperatures measured for the low-beam are consistently higher than those for the high-beam. As the heat release is similar in both cases, this could be explained by the fact that whereas the latter is vented with fresh air, the former receives warm air. The internal communication between high- and low-beam areas instigates this stream of warm air entering the low-beam cavity laterally from the neighboring space. In addition, the larger size of the light bulb in the low-beam further contributes to the higher temperatures mentioned above. In brief, maximum measured temperatures were 149.5 °C and 124.3 °C for the low- and high-beams, respectively.

Fig. 6b and c suggests that the observations made previously regarding the main reflector apply to the secondary reflectors as well. Again, the higher wall temperatures were measured on the top surfaces of the reflectors. Taking into account that temperatures clearly above 100 °C were registered in these areas, and the close proximity of the front lens, it is easy to understand the choice of semi-transparent polycarbonate (as opposed of polymethyl methacrylate for example) as the material for this component. In contrast, the results show that the lower surfaces of both headlight cavities remain somewhat cooler for the investigated conditions, with temperatures typically being around 50 °C.

3.3. Fluid flow structure

The structure of the fluid flow velocity field inside the headlight cavities was characterized for the steady operating conditions described in the previous subsection. Simultaneous measurement of time-averaged values for

the three velocity components was carried out in several vertical (Y, Z) planes, in accordance with the coordinate system defined in Fig. 1a. It must be noted that, for the sake of simplicity, the spatial coordinates are always referenced to the location of the light bulb filament in each cavity. As the filaments are several millimeters long, the X-coordinate reference was defined by prescribing the distance to the surface of the front lens along this axis: 107.0 mm for the high-beam and 126.4 mm for the low-beam.

Tentative measurement grids were initially defined at the selected planes based on the design dimensions of the headlight alone. However, due to the occurrence of direct/diffuse reflections and unforeseen blocking of the laser beams at some locations, several modifications to the base grids have been made. Before the accomplishment of the measurements, a sweep through all grid points had to be carried out in order to assess the signal quality and laser reflection hazards. The final results are portrayed in Figs. 7a–c and 9a–c, for the high- and low-beams respectively. In these figures, in-plane velocities (V, W) are illustrated as vectors, whereas the out-of-plane velocity component (U) is shown in grey scale contours obtained from irregularly distributed data points by triangulation. An inset is included in each figure displaying a middle section cut from both main and secondary reflectors. The dotted line indicates the relative position of the various measurement planes.

The measurements presented in Fig. 7a represent a plane crossing the light bulb of the high-beam, which explains the circular blank area in the origin of the axes. The thermal plume formed above the heat source is

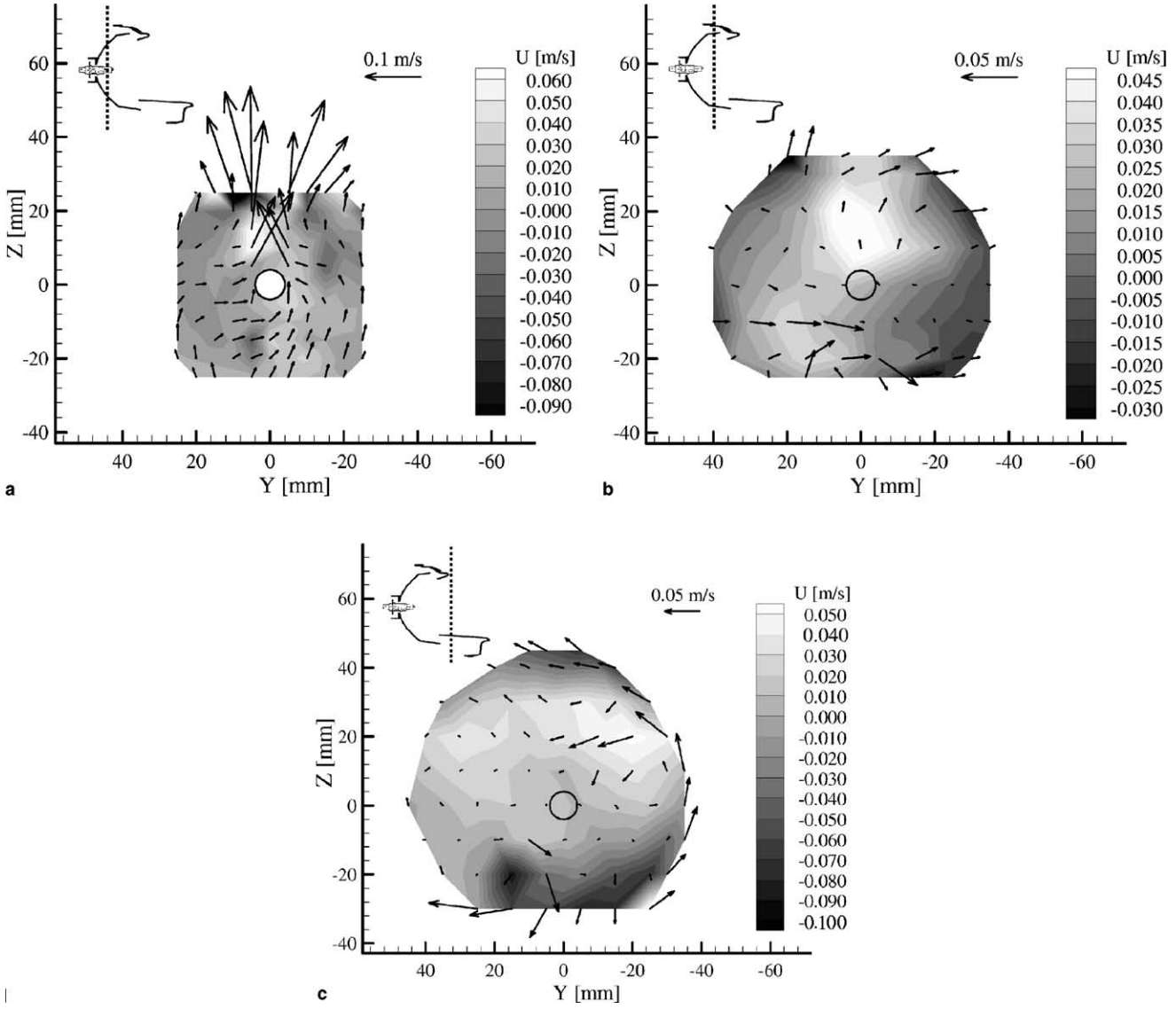

Fig. 7. Fluid flow velocities in vertical planes inside the high-beam cavity for steady operating conditions. (a) $X = 0$ mm, (b) $X = -24$ mm, and (c) $X = -64$ mm.

clearly identified by the large vertical velocities of the fluid in this region. The relatively cold fluid entering through the venting aperture (lower left-hand side) is convected upwards and around the glass bulb where, in contact with an extremely hot surface, it experiences a steep acceleration. Consequently, the velocity gradient across the plume is high, as observed by Barozzi and Corticelli (2000) in their two-dimensional numerical simulations. As the present case is three-dimensional, a significant amount of fluid is also directed perpendicularly to the plane of the measurements and into the region above the heat source. Moving in the direction of the front lens, at a distance of 24 mm from the bulb filament this effect has spread to a wider area in the central region of the cavity, as shown in Fig. 7b. On the other hand, at this intermediate section, the in-plane velocities mainly indicate flow from left to right (top right and bottom). This is undoubtedly associated with the lateral communication between high- and low-beam cavities referred to in Section 2.1.

Further away from the main reflector, at a distance of 64 mm from the bulb filament, the pattern exhibited by the contours of U-velocity discloses a very important feature of the flow. The third measurement plane shown in Fig. 7c testifies that the fluid on the top and on the bottom of the cavity moves in the direction of the lens (negative U-velocities), whereas the fluid in the layer in between is flowing in the opposite direction (positive U-velocities). This is a clear indication of the establishment of two large Y-axis vortices, one on top of the other. In addition, the figure also suggests that a significant fraction of the fresh fluid aspirating through the vent flows around the back surface of the secondary reflector, passes in the gap between secondary and main reflectors and emerges at the lower left corner of the cavity. At this location, the fluid is gushing out at high speed (large negative U-velocities) towards the front lens. This effect seems to explain why the lowest wall temperatures were measured in this area (see Fig. 6b). In contrast, the flow on the upper region of the cavity brings the hot fluid directly towards the lens, which is potentially problematic. In-plane velocities indicate that the above-mentioned jet of fresh fluid contiguous to the lower surface of the secondary reflector gains clockwise swirl (X-axis rotation), most likely due to the change in fluid direction around the reflector edge. Furthermore, part of this layer of cold fluid travels to the right-hand side along the aforementioned wall, rises along the border of the reflector and most likely then merges with the central stream towards the rear zone of the high-beam cavity. Fig. 8 shows a schematic representation of these circulations showing the approximate location of the vent as well.

The first measurement plane inside the low-beam cavity intersects the corresponding light bulb. In this case, the blank area shown in Fig. 9a denotes the cross-section of the metallic screen installed in front of the bulb (previously mentioned). At this X-position, the flow presents many similarities with the reciprocal plane measured in the high-beam cavity. The principal differences may be summarized as follows. Firstly, the magnitudes of the buoyancy velocities in the thermal plume are smaller, mostly as a consequence of the higher temperature of the surrounding mass of air. This is in agreement with the findings of Abib and Jaluria (1995) who concluded that the thermal stratification reduces the buoyancy level, resulting in a weaker penetrative capability of the plume. The presence of the metallic screen contributes further to the occurrence of lower velocities. Secondly, the location of the fastest stream flowing perpendicularly to the plane (towards the surface of the main reflector) has moved to the left of the heat source. An explanation can be found by noting that all the fluid entering the cavity emanates from that side as well. The aforementioned lateral flow can also be observed in a measurement plane situated at a distance of 31 mm from the bulb filament, in the direction of the front lens. In fact, fluid infiltrating the low-beam cavity displays large V- and U-velocity components, as shown in Fig. 9b. However, the development of strong out-of-plane motion in this flow is fundamentally due to the concave surface of the main reflector. In addition, it can be seen that the fluid moves in the direction of the heat source, changing its trajectory upward by approximately 45° upon heating up. Part of this hot air stream then exits the headlight enclosure through the outlet vent (upper right-hand corner) while the remainder keeps on recirculating inside the cavity.

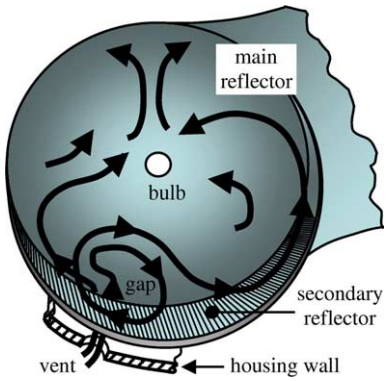

Fig. 8. Schematic view of the circulations inside the high-beam cavity.

The U-velocity contours in the upper area of the cavity strongly suggest the formation of two adjacent, Y-axis vortices. This is, once more, a consequence of the fluid negotiating the curved boundary of the main reflector. On the other hand, the large region on the lower right-hand side of this cavity seems to be filled by nearly stagnant fluid, which contrasts with the considerable motility of the remaining volume. The proximity of

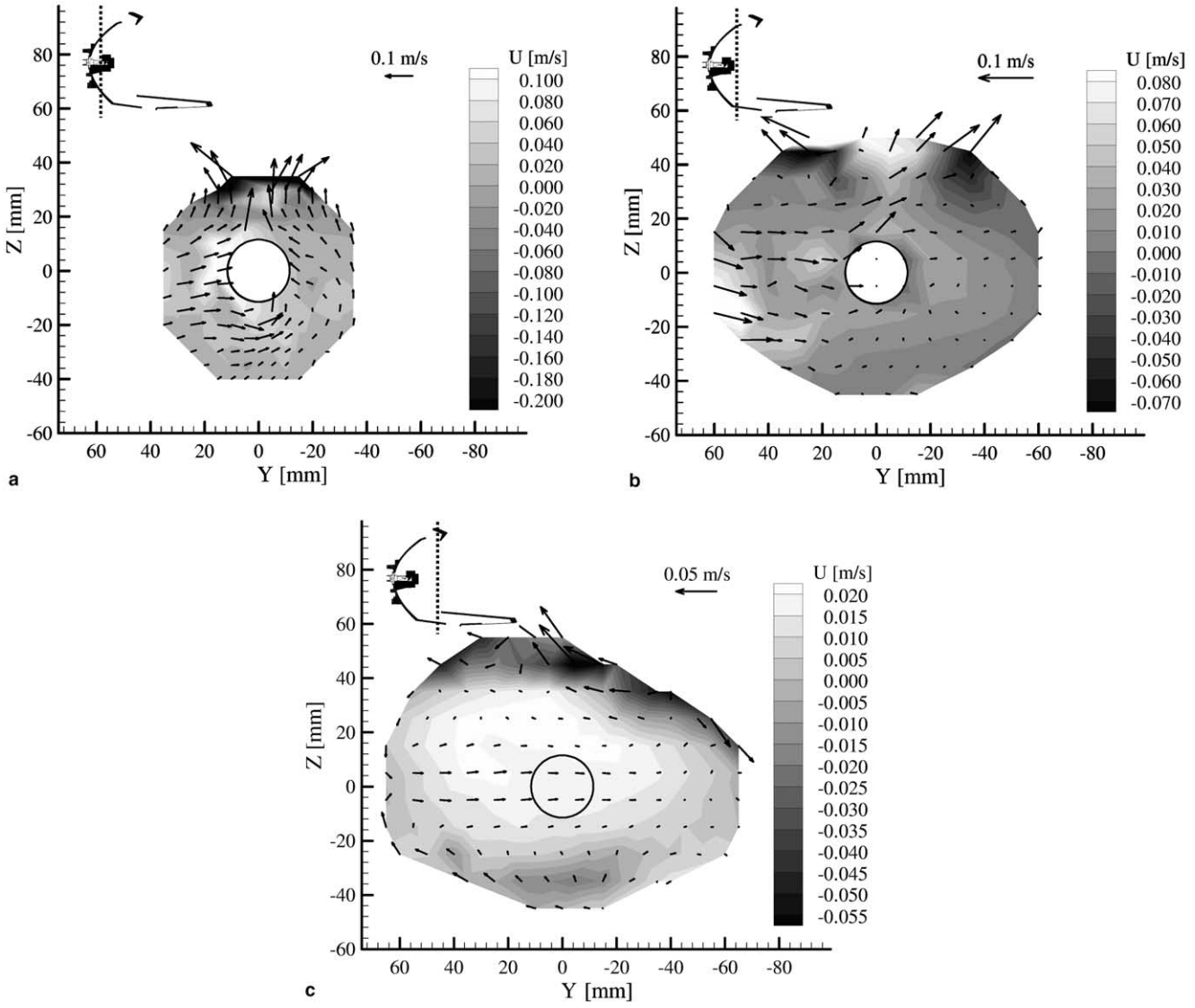

Fig. 9. Fluid flow velocities in vertical planes inside the low-beam cavity for steady operating conditions. (a) $X = 0$ mm, (b) $X = -31$ mm, and (c) $X = -71$ mm.

the heat source creates a barrier which minimizes the exchange of fluid between both sides of the cavity.

Perhaps the most interesting topological feature of the flow is again revealed by the measurement plane located closer to the front lens. Fig. 9c depicts these results, obtained at a distance of 71 mm from the bulb filament. In this case, the establishment of a fluid structure containing two large Y-axis vortices and occupying the full vertical extent of the cavity is even more unmistakable.

The development of a vortex-dominated flow instead of a wall boundary layer regime inside a square enclosure with an internal heat source (located in a bottom corner) was computationally predicted by Sun and Emery (1997) for the condition $Ra'/Ra \gg 1$. The present investigation has corroborated this aspect of their numerical predictions and the formation of a double vortex structure may, in this case, be explained by the elevated position of the heat source.

4. Summary and conclusions

An experimental investigation of fluid flow and wall temperature distributions in automotive headlight has been conducted employing laser-Doppler velocimetry and thermocouple thermography. The subject of the study was a front lighting unit designed with single housing and a clear double lens. It included low- and high-beam lamps, turn-signal lamp and parking lamp. Transient measurements of wall temperatures were carried out first with the objective of determining the characteristic heat-up time of the headlight. Subsequently, steady operating conditions were characterized

measuring both the wall temperatures and the three-dimensional time-averaged flow field inside the headlight cavities.

It was found that a significant thermal stratification occurs in the headlight cavities, locally rising the temperature of upper inner surfaces to values well beyond 100 °C. This fact presents a challenge for the designers of modern lightweight plastic-made headlights. On the other hand it was observed that the regime corresponding to steady operating conditions ($Ra'/Ra \gg 1$) is characterized by the development of a vortex-dominated flow. The velocity measurements for both the high- and low-beam cavities have illustrated the formation of two vertical vortices of large dimensions, one on top of the other. This topology is consistent with the occurrence of natural convection inside an enclosure containing an elevated heat source. In addition, it was concluded that the interaction of the main vortex flow with the stream of colder fluid entering the enclosed volume through the venting aperture cannot be neglected because it contributes significantly to increase the complexity of the basic flow pattern.

References

Abib, A.H., Jaluria, Y., 1995. Penetrative convection in a stably stratified enclosure. International Journal of Heat and Mass Transfer 38 (13), 2489–2500.

Albrecht, H.-E., Borys, M., Damaschke, N., Tropea, C., 2003. Laser Doppler and Phase Doppler Measurement Techniques. Springer-Verlag, Berlin, Heidelberg.

Barozzi, G.S., Corticelli, M.A., 2000. Natural convection in cavities containing internal sources. Heat and Mass Transfer 36 (6), 473–480.

Bejan, A., 1984. Convection Heat Transfer. Wiley, New York.

Bielecki, J.W., Chang, M., Poorman, T., 2003. The effect of environmental conditions on moisture clearing time in automotive lamps. SAE Paper No. 2003-01-0646.

Buchhave, P., George Jr., W.K., Lumley, J.L., 1979. The measurement of turbulence with the laser-Doppler anemometer. Annual Review of Fluid Mechanics 11, 443–504.

Chenevier, C., 2001. Thermal simulation in lighting systems—5 days/5 degrees. In: Proceedings of the Fourth International Symposium Progress in Automotive Lighting, Darmstadt, Germany, pp. 109–118.

Erdmann, J.C., Tropea, C.D., 1981. Turbulence-induced statistical bias in laser anemometry. In: Proceedings of the Seventh Biennal Symposium on Turbulence, Rolla, Missouri.

Halgren, C.T., Hilburger, F.K., 2003. Development and correlation of internal heat test simulation using CFD. SAE Paper No. 2003-01-0647.

Huhn, W., 2002. Proposal for a lighting strategy—The car makers point of view. SAE Paper No. 2002-01-0528.

Incropera, F.P., 1988. Convection heat transfer in electronic cooling. ASME Journal of Heat Transfer 110 (11), 1097–1111.

Jue, T.C., 2003. Analysis of thermal convection in a fluid-saturated porous cavity with internal heat generation. Heat and Mass Transfer 40 (1–2), 83–89.

Küpper, L., Schug, J., 2002. Active night vision systems. SAE Paper No. 2002-01-0013.

Moore, W.I., Powers, C.R., 1999. Temperature predictions for automotive headlamps using a coupled radiation and natural convection model. SAE Paper No. 1999-01-0698.

Moore, W.I., Donovan, E.S., Powers, C.R., 1999. Thermal analysis of automotive lamps using ADINA-F coupled specular radiation and natural convection model. Computers and Structures 72 (1), 17–30.

Okada, Y., Nouzawa, T., Nakamura, T., 2002. CFD analysis of the flow in an automotive headlamp. JSAE Review 23 (1), 95–100.

Shiozawa, T., Yoneyama, M., Sakakibara, K., Goto, S., Tsuda, N., Saga, T., Kobayashi, T., 2001. Thermal air flow analysis of an automotive headlamp: the PIV measurement and the CFD calculation for a mass production model. JSAE Review 22 (2), 245–252.

Sun, Y.S., Emery, A.F., 1997. Effects of wall conduction, internal heat sources and an internal baffle on natural convection heat transfer in a rectangular enclosure. International Journal of Heat and Mass Transfer 40 (4), 915–929.

Wulf, J., Reich, A., 2002. Temperature loads in headlamps. SAE Paper No. 2002-01-0912.

Yerkes, K.L., Faghri, A., 1992. Mixed convection analysis in large baffled rectangular chambers with internal heat-sources. International Journal of Heat and Mass Transfer 35 (5), 1209–1228.